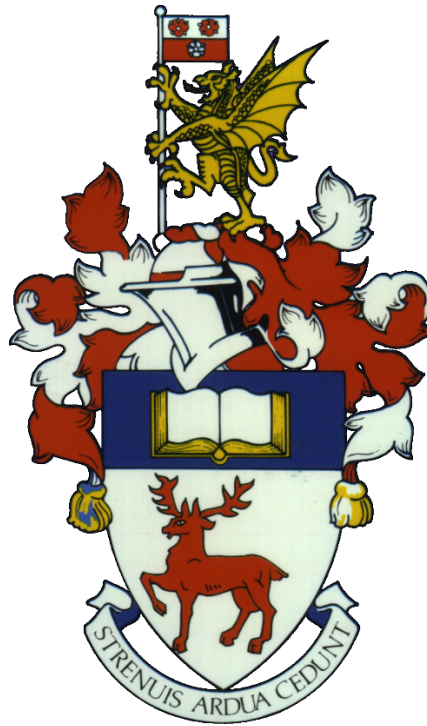


UNIVERSITY OF SOUTHAMPTON

FACULTY OF ENGINEERING AND PHYSICAL SCIENCES  
SCHOOL OF ENGINEERING  
MARITIME ENGINEERING AND SHIP SCIENCE



**Individual Project:**  
**Investigation of the Influence of Crew Setup on  
Performance for the Olympic NACRA 17 Foiling  
Catamaran**

**Author:**  
**Louis HUCHET**  
huchetlouis@gmail.com

**Faculty Advisor:**  
**Professor Stephen R. Turnock**  
S.R.Turnock@soton.ac.uk

April 2021

**SUMMARY** A critical part of preparing sailing races is to understand how best to set up a yacht so that it can race as fast as possible in the desired direction. With the arrival of hydrofoils in the Olympic Class catamaran in 2016 on the Nacra 17, sailing has gone more complex with the possibility of sailing both in displacement and foiling modes. Numerical tools are nowadays necessary to help sailors in their preparation and understand how to setup their boat to maximise their chances of winning. A Velocity Prediction Program (VPP) was developed on Python to investigate the key parameters playing a role in the overall performance, including the weight of the crew and their longitudinal position on the hull. Given an initial set of environmental conditions, foil settings and sails area, the VPP uses the balance of forces to find the optimum boat speed for each wind speed and yacht direction. Three different crew weights are analysed: 120, 150 and 180kg, as well as longitudinal positions comprised between 0.5 and 1.8m away from the transom. The results are presented in the form of polars and validated by comparing them to real-life sailing data, as well as polar diagrams obtained using more advanced methods such as CFD. The results show that in winds below 10 knots, the lighter crew has an advantage over heavier crews as they are able to foil in a wider range of headings while sailing downwind. In stronger winds, the heavier crews are advantaged as they can withstand more power when foiling. Similarly, crews that are far aft on the hull can switch to a foiling mode more quickly when sailing closer to the wind as it enables to increase the foil's angle of attack and avoid nose-diving. The VPP uses optimisation functions and investigates the abilities of the Nacra 17 to foil and sail in the direction of the wind (VMG).

## Contents

<b>1</b>	<b>Introduction</b>	<b>3</b>
1.1	Introduction . . . . .	3
1.2	Aim . . . . .	3
1.3	Objectives . . . . .	3
<b>2</b>	<b>Background</b>	<b>3</b>
2.1	Sailing Background . . . . .	3
2.1.1	Basic physics . . . . .	3
2.1.2	Aerodynamic Force . . . . .	4
2.1.3	Hydrodynamic forces . . . . .	4
2.1.4	Balance of forces in motion . . . . .	5
2.2	Nacra 17 . . . . .	6
2.2.1	The platform . . . . .	6
2.2.2	Pitch Stability . . . . .	7
2.2.3	Heave stability . . . . .	8
2.3	Performance Prediction . . . . .	8
2.3.1	Overview . . . . .	8
2.3.2	Aerodynamic model . . . . .	9
2.3.3	Hydrodynamic model . . . . .	9
<b>3</b>	<b>Mathematical Approach</b>	<b>10</b>
3.1	Flow chart and numerical method . . . . .	10
3.2	Aerodynamic Model . . . . .	11
3.2.1	Wind triangle . . . . .	11
3.2.2	Sail Force Model . . . . .	11
3.2.3	Windage . . . . .	12
3.3	Hydrodynamic Model . . . . .	13
3.3.1	Hull resistance . . . . .	13
3.3.2	Flying condition . . . . .	13
3.4	Numerical program processing . . . . .	15
<b>4</b>	<b>Results &amp; Discussions</b>	<b>15</b>
4.1	Presentation of Polar Diagrams . . . . .	15
4.2	Comparison of VPP . . . . .	16
4.2.1	Elapsed time on a typical windward-leeward race course . . . . .	16
4.2.2	Comparison with the <i>Journal of Sailing Technology</i> . . . . .	17
4.3	Influence of crew weight and crew position on performances . . . . .	18
4.3.1	Crew weight investigation . . . . .	18
4.3.2	Longitudinal crew position investigation . . . . .	19
4.4	Limitations . . . . .	19
<b>5</b>	<b>Conclusion</b>	<b>20</b>
<b>6</b>	<b>Appendix</b>	<b>22</b>

## Nomenclature

$(1 + k)$	Form factor	
$\alpha$	Foil's angle of attack	[ $^{\circ}$ ]
$\beta$	Apparent Wind Angle	[ $^{\circ}$ ]
$\Delta$	Displacement	[ $N$ ]
$\gamma$	True Wind Angle	[ $^{\circ}$ ]
$\rho_{air}$	Air density	[ $kg/m^3$ ]
$\rho_{water}$	Water density	[ $kg/m^3$ ]
$A_G$	Aspect ratio	
$A_w$	Hull's wetted surface area	[ $m^2$ ]
$A_{proj}$	Foil's projected area	[ $m^2$ ]
$A_{wetted}$	Foil's wetted area	[ $m^2$ ]
$c$	Foil's chord	[ $m$ ]
$C_D$	Drag Coefficient	
$C_f$	Friction coefficient	
$C_L$	Lift Coefficient	
$C_R$	Residuary Coefficient	
$C_{D0}$	Viscous drag coefficient	
$C_{D_P}$	Pressure drag coefficient	
$C_{D_i}$	Induced drag coefficient	
$C_{D_{spray}}$	Spray drag coefficient	
$C_{D_w}$	Wavemaking drag coefficient	
$D$	Drag	[ $N$ ]
$D_A$	Windage	[ $N$ ]
$D_{spray}$	Spray drag	[ $N$ ]
$F_x$	Driving force	[ $N$ ]
$F_y$	Side force	[ $N$ ]
$g$	Acceleration of gravity	[ $m/s^2$ ]
$L$	Lift	[ $N$ ]
$R_h$	Hydrodynamic drag	[ $N$ ]
$Re$	Reynolds number	
$S$	Foil's span	[ $m$ ]
$S_{sail}$	Area of the sail	[ $m^2$ ]
$t$	Foil's thickness	[ $m$ ]
$V_A$	Apparent Wind Speed	[ $m/s$ ]
$V_S$	Boat Speed	[ $m/s$ ]
$V_T$	True Wind Speed	[ $m/s$ ]
$W$	Weight	[ $N$ ]
$x_{crew}$	Longitudinal position of the crew	[ $m$ ]
$y_{rh}$	Foil's depth of immersion	[ $m$ ]
$z$	Vertical distance between the aerodynamic and hydrodynamic centres of effort	[ $m$ ]

# 1 Introduction

## 1.1 Introduction

One of the novelties in the mixed-crew multihull Olympic Class, is the addition of hydrofoils. Since the replacement in 2016 of the Tornado by the Nacra 17 as the new Olympic Class catamaran, sailors have consistently trained to sail faster by handling as best as possible the new foiling daggerboards and use them as their advantage to improve their performances in a fleet race. Allowing the Nacra 17 to sail both in displacement and foiling mode, these hydrofoils actively increase the complexity of sailing and demand a higher level in keeping the boat at high speeds.

Due to a larger number of parameters to handle while sailing at high speeds, the aim is therefore to bring the sailors a numerical tool predicting the performances of the Nacra 17, both in displacement and foiling modes, to aid them get a better understanding of its behaviour. A Python-based Velocity Prediction Program (VPP) is developed by balancing the forces and moments acting on the catamaran and aims to find the optimum speed that can be achieved by investigating the influence of crew setup in steady-state<sup>1</sup> conditions. The crew setup investigated in this report is a combination of both weight (120, 150 & 180kg) and longitudinal position (comprised between 0.5m and 1.8m from the transom) of the crew on the hull.

To achieve this, a thorough analysis of the physics happening on a sailboat is necessary to understand the parameters impacting the performance. The Nacra 17's platform is then studied to understand its different components that can be implemented in the VPP process. It is of crucial importance to develop accurate force models and mathematically transcribe them in the numerical program to get accurate results. The VPP is validated by comparing the results to real-life data and CFD-based VPP results published in the *Journal of Sailing Technology* [22]. Once validated, the VPP is used to investigate the influence of crew setup on performances, as reflected in the title.

## 1.2 Aim

To bring Nacra-17 sailors a tool that helps them find the optimum setup to increase their speed and performances given a set of environmental conditions.

## 1.3 Objectives

- i Investigate the parameters contributing to the performance of a sailing yacht.
- ii Investigate the mode of operation of a conventional VPP.
- iii Develop a performance prediction numerical tool adapted for the Nacra-17.
- iv Develop accurate models simulating the forces acting on a Nacra-17.
- v Develop accurate numerical tool on Python predicting theoretical speeds of Nacra 17, with associated parameters
- vi Analyse the influence of crew setup on the Nacra-17 performances.

# 2 Background

The physics and the necessary knowledge to understand the motion and the equilibrium of a yacht in motion provided in this section are mainly based on [12], [13] and [19].

## 2.1 Sailing Background

### 2.1.1 Basic physics

The motion of a sailing yacht between two fluids of different density (water and air) is the result of the action of a number of forces which come from the fluids flowing around the yacht's elements (hull, sails, appendages. . .). Because there are two fluids, two different types of forces need to be considered: hydrodynamic and aerodynamic. The interaction between these two resulting forces determines the heading of the boat and how fast it will be going. From Newton's law, when the boat is moving in a stable manner and with a constant velocity, the forces acting on the yacht are in equilibrium. These forces acting at different origins, and in different directions, the sailing yacht therefore undergoes dynamic momentum and operates in a number of Degrees of Freedom (DoF).

This 'mechanical view' of the sailing yacht, also considered as a 'physical system' in [12] needs a coordinate system and a reference point in order to interpret its motion and behaviour between the wind and sea. To describe this motion, six fundamental types of motions must be considered. The first three involve rotational motion around particular axes, while the other three involve linear motion (see figure 1). Since the yacht operates in six degrees of freedom, six dynamic equations will be needed to describe its motion. For simplicity, these equations are only investigated later on and only

---

<sup>1</sup>Meaning the initial conditions do not change with time

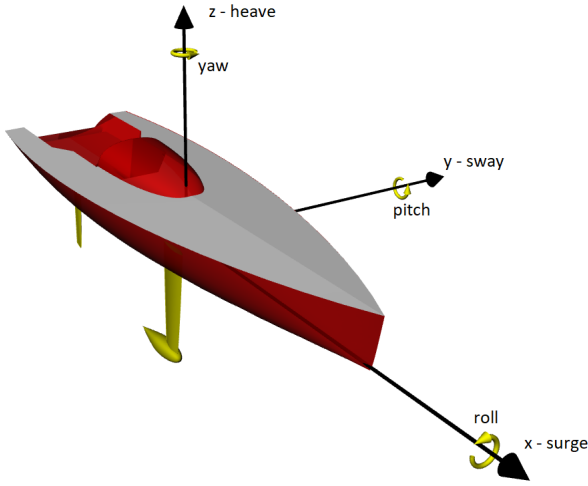


Figure 1: Degrees of freedom of a boat

the effects of the forces applied on the motion of the yacht are considered for now.

A third force component not relating to the aerodynamic or hydrodynamic forces is caused by the weights of the boat and crew. On dinghies (i.e. small sailing open boats), the weight of the crew can be equal, or perhaps greater than that of the boat itself and therefore have a significant influence upon the stability. This influence will be investigated later on in this report. The two sections below illustrate separately the two resulting aerodynamic and hydrodynamic forces respectively.

### 2.1.2 Aerodynamic Force

Aerodynamic force is generated by one or more sails. A photo of the sails is shown below where the main sail (big rear sail), the jib (small sail) and the spinnaker (big blue sail) are hoisted. The latest is only used in certain courses (downwind) to maximise the driving force and therefore increase the speed. Sails are acting like wing planes and generate lift and drag in the vertical plane, which result in a lateral force perpendicular to the direction sailed and a driving force acting along the direction sailed.

Just like wings, the shape of the sails can be adjusted with sheets<sup>2</sup> in order to increase the camber<sup>3</sup>, the angle of attack<sup>4</sup> or the twist<sup>5</sup> which all have an influence on the lift and drag generated by the air flowing around the sails. When added together in the horizontal plane (parallel to the water surface), these forces compose the total aerodynamic force. A single point over the surface of the



Figure 2: Nacra 17 sailing downwind with the main sail, the jib and the spinnaker in Auckland for the World Championship, 2019 ©Sailing Energy

sails can be modelled as the Centre of Effort (CE) at which the total force of the wind would produce an identical force in modulus and direction with that produced by its distribution over the whole sail. It is usually assumed that the centre of effort is the geometrical centre of the sail area. However, the actual position of this point is a function of a whole series of variables, including the way in which the yacht's sails are trimmed.

A third aerodynamic force needs to be accounted for in the balance of forces, that is the windage. It includes all the drag forces generated by the non-lifting components of the boat (e.g. hulls, trampoline, crew, rigging, etc.).

### 2.1.3 Hydrodynamic forces

If the situation below the waterline is now analysed, the appendages and the hulls play an analogous role to that of the sails. In fact if the boat would generate no other forces than the ones above the waterline, the boat would just follow the direction of the total aerodynamic force. As mentioned in [12], over the keel, rudders, and the bottom of the boat there is a flow in relative motion and they behave as if they were the 'wings' of an aeroplane 'flying' in the water. The result of this interaction between the hull and the water surrounding it is the creation of a hydrodynamic force applied to a point called the Centre of Lateral Resistance (CLR). Because of the side-force generated by the sails, the boat will be deviated downwind by an angle called the 'lee-way angle'. This angle thus represents the angle of attack with which the water flows around the hull and appendages. Just like the air flowing over a wing, the water flowing around the hull and its appendages will generate lift and drag which results

<sup>2</sup>Nautical terms for "ropes"  
<sup>3</sup>Measures the fullness, or depth of the sail  
<sup>4</sup>Angle at which the sail is adjusted with respect to the apparent wind  
<sup>5</sup>Change in the angle of attack from the bottom of the sail to the top of the sail

in a force that will oppose the aerodynamic and prevent the boat from drifting. When the boat is underway, the aerodynamic forces must balance the hydrodynamic forces. In other words, the motion of the yacht (and hence its performance) is governed by the dynamic equilibrium of the forces applied to it. On a catamaran such as the Nacra 17, the yacht is composed of two parallel thin hulls joined by cross-beams with one rudder and one curved daggerboard - called hydrofoil - attached to each hull. The origin of the hydrodynamic drag can be broken down into a number of different parts such as the resistance when the boat is sailing upright, the additional resistance when the boat is heeled or the resistance developed when the action of the wind on the water creates waves. Further breakdown of the total resistance is described in section 2.3.3 to understand the various mechanisms that take part in the dynamic equilibrium.

### 2.1.4 Balance of forces in motion

The sketches below sum up the balance of forces applied to a conventional yacht in the X-Y plane and in the Z-X plane. The study of the yacht's behaviour is governed by how these forces interact with each other when the yacht is in motion.

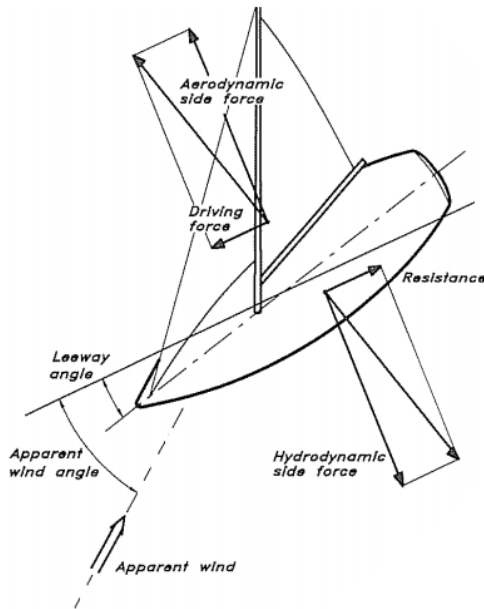


Figure 3: Balance of forces on a conventional yacht in the horizontal (X-Y) plane from [10]

When in motion, the wind experienced by the sails is the combination of the wind produced by the speed of the boat itself and the true wind speed. The combination of both winds is called the 'apparent wind' - vector  $V_A$  in the sketch below (figure 5). Therefore, from the true wind (vector  $V_T$ ) data and a given boat speed and direction (vector  $V_S$ ), it is

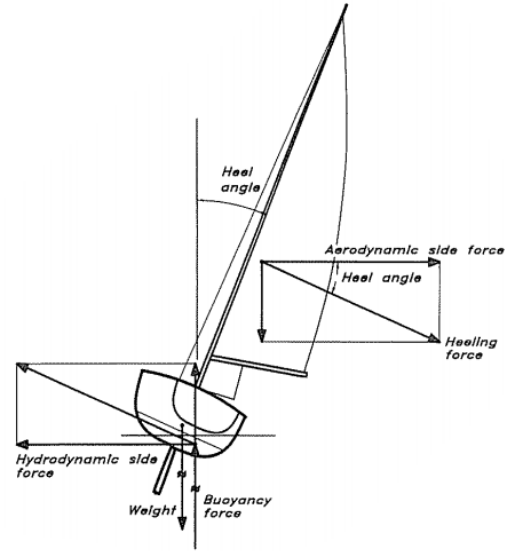


Figure 4: Balance of forces on a conventional yacht in the vertical plane (Z-Y) from [10]

possible to determine the angle and the speed of the wind experienced by the sails, and therefore be able to trim them properly.

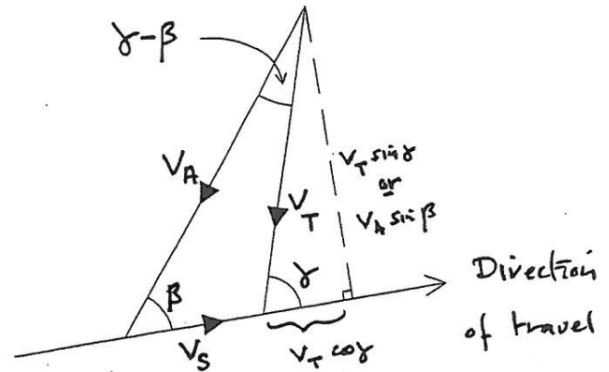


Figure 5: Wind Triangle Phenomenon [19]

Sails therefore generate forces with components perpendicular to the apparent wind, that is lift, which have a great importance in studying the behaviour of a sailing boat. Similarly, as concerns the submerged part of the boat, from an analysis of figure 3, it can be seen that the total hydrodynamic force developed by the submerged part is not fully useful in driving the boat along. In fact, as mentioned earlier, this force can be broken down into components acting in the opposite direction of the boat's heading called the hydrodynamic resistance, which tends to have the effect of slowing the boat. The equation of balance between the aero and hydrodynamic forces is a vector equation and as such, on a plane, can be broken down into two scalar equations representing the equilibrium of the components of these forces in two set directions. It is therefore clear to state in the water surface

plane (horizontal), in steady-state conditions, that is when there is no variations in boat and/or wind speed, either in direction or modulus, the total hydrodynamic resistance  $R_T$  must balance the aerodynamic driving force  $F_x$  in the heading direction ; and the aerodynamic side force  $F_y$  must balance the hydrodynamic side force  $F_h$  in the direction perpendicular to the heading. This gives rise to the following system of equation that governs the equilibrium condition:

$$R_t = F_x \quad (1)$$

$$F_y = F_h \quad (2)$$

As shown in figure 4, since aerodynamic and hydrodynamic forces are applied at a certain height above or below the waterline, it produces a moment that tends to make the boat heel. The aerodynamic heeling force not only pushes the boat sideways but also has the effect of creating a heeling couple on the boat that tends to incline it to leeward. This is also true for the hydrodynamic lift applied to the lateral centre of resistance CLR that is at certain height below the waterline. The side force generated by the appendages not only counteracts leeway, but also creates a Heeling Moment (HM) working on the boat that tends to make it heel to leeward too. This heeling moment is balanced by the righting moment (RM) deriving from the fact that, when the boat heels, the weights  $W$  from the crew and the boat and the buoyancy force  $\Delta$ , although they balance each other, act in two straight lines separated by a distance which depends on the degree of heel. Therefore, in the vertical plane, perpendicular to the water surface, these two moments must balance each other to be in equilibrium. If the heeling moment is too important, the boat capsizes. From this equilibrium investigation, a better understanding of how sailing yachts behave have been achieved and allows to investigate the laws governing the motion and the dynamic behaviour of a foiling catamaran in greater depth.

## 2.2 Nacra 17

### 2.2.1 The platform

The Nacra 17 is a 17-foot catamaran which has been chosen in 2012 as the new equipment for the mixed multihull event for the 2016 Rio-de-Janeiro Olympic games. It replaces the Tornado which had been the Olympic class catamaran since 1976. According to the Class, the Nacra 17 was purposely designed by Pete Melvin and Gino Morelli (founders of Morelli & Melvin, New-Zealand) from

scratch to meet the design criteria imposed by the International Sailing Federation (ISAF ) [21]. For the first edition in 2016, they chose to equip the new catamaran with curved daggerboards (constant curvature along the whole span<sup>6</sup>) which was a relatively new technology back then. In fact, these C-foils allow to sail in a normal catamaran configuration (i.e. the leeward hull in the water and the windward hull off the water) and in a foiling configuration. The foiling configuration, which implies the boat is “flying” with both hulls above the water, greatly reduces the wetted area of the hulls. Therefore, it is necessary for the crew to enhance this condition in order to improve the performance.[20]

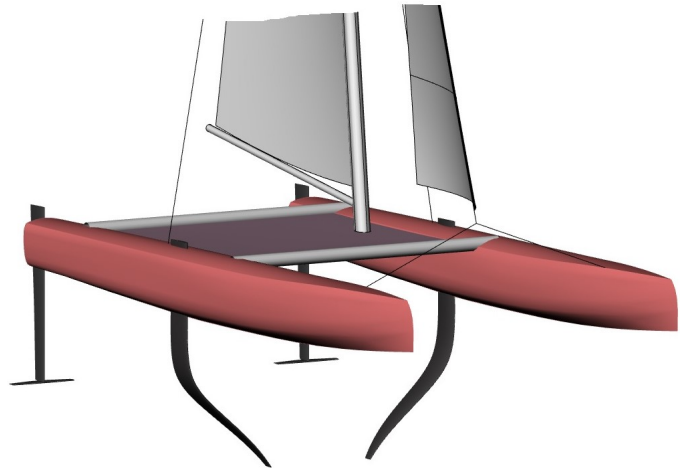


Figure 6: 3D render of the Nacra 17 - created by superimposition

Further improvements were made for the next Tokyo Olympic Games (originally in 2020, though postponed to 2021 due to the international pandemic). In fact, the Class and ©Nacra Sailing agreed to evolve the boat to become a fully foiling catamaran. The transition occurred to a 4-point fully foiling multihull. The hulls had therefore the option to retrofit themselves into the fully foiling configuration. This new version of the catamaran is called the “MK-II” and this paper therefore deal with this version where the design characteristics can be found in table 1.

A 4-point fully foiling catamaran therefore means the 4 Z-shaped foils need to remain in low position at all time in order to achieve adequate lift and heave stability, as well as safety as the crew do not have to raise and lower the daggerboards at each tack or gybe and thus allow faster maneuvers. In this report, as the foils data were not publicly available, the foils were modeled based on several assumptions. From the update configuration presented by Pete Melvin in 2016 [15], some significant

<sup>6</sup>Distance from one foil tip to the other

Table 1: Nacra 17 particulars

Length Overall (LOA)	5.25 m
Waterline Length (LWL)	5.15 m
Overall Beam	2.59 m
Hull beam	0.40 m
Boat weight (dry condition)	163 kg
Sailing weight	171 kg
Opt. crew weight	120-140 kg
Mainsail area	16.1 m <sup>2</sup>
Jib area	4.0 m <sup>2</sup>
Spinnaker area	17.9 m <sup>2</sup>
Rig height from Design Waterline (DWL)	9.56 m

data such as the span and the profile shape were used. Only assumptions on the section profile were made. In fact, in 2017, within the faculty of Engineering and physical science of the University of Southampton, a group of Master students outlined the design and manufacture process of a Nacra F18 foiling test platform [16]. A 3D scan of the foils was realised and the closest comparable NACA<sup>7</sup> section that matched the foils was a NACA-2416 profile. Therefore, it is assumed in this report that the Nacra17-MKII uses the same section profile on its foils. Moreover, from comparison and sketches available online, the chord was found to be 0.238m. The design characteristics are described in table 2.

From comparison and publicly available information, a 3D-model of the Nacra 17 was created in order to get more geometric data such as the hulls wetted area for the resistance data, or the wetted and projected areas relative to the depth immersion<sup>8</sup> for the foils. The foils were modeled using an excel-driven ©Solidworks developed by S. Haściłowicz [23] at the University of Southampton in which the shape and the profiles were loaded. A photo of the model is shown in figure 6.

Table 2: Foils particulars

Profile	NACA-2416
Span, $S$	1.9 m
Chord, $c$	0.238 m
Thickness, $t$	0.0381 m
$t/c$	0.16

### 2.2.2 Pitch Stability

The pitch stability is governed by the interaction between the forces acting in the x-z plane. These forces acting at different origins create moments that will impact the pitch stability. A free-body diagram summarizing the forces acting in this plane

is shown in figure 7. It is noticeable to say that the longitudinal position of the foils and the crew have a great influence on the moments created and thus on pitch stability. According to the class rule, the foil’s rake angle<sup>9</sup> cannot be adjusted throughout a race and it is therefore the crew that needs to move forward or backward to adjust the equilibrium of forces and find an optimum angle where the boat is stable. The levers of the forces relative to the reference point (center of gravity of the catamaran) are referenced in table 3. The initial centre of effort of the sails is assumed to be the geometrical centre of area, which is approximately 40% of the luff<sup>10</sup> height, thus 3.8m. In fact, it will be shown that the CE height can be modified through certain variables. Moreover, the origin of total resistance may vary depending on whether the boat flies because of the resistance of the hull. Though when flying, the point of application remains approximately at half the immersion depth and thus remains constant in relation to the reference point. The crew is assumed to be furthest aft in order to calculate the maximum driving force that the boat can support before nose diving. Similarly, it will be shown that the lift generated by the elevator - small lifting surface on the rudder serving as a stabilizer - can be negative to meet the equilibrium conditions and avoid nose diving.

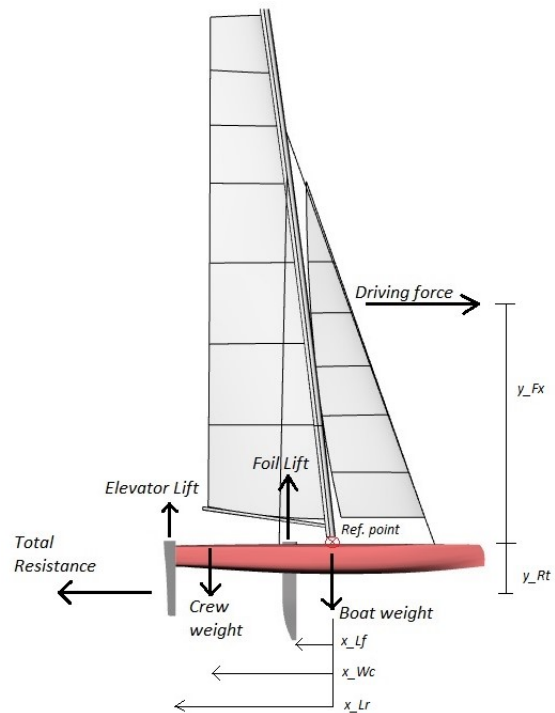


Figure 7: Longitudinal free-body diagram for pitch stability study

<sup>7</sup> Airfoil shape developed by the National Advisory Committee for Aeronautics

<sup>8</sup> Vertical distance from the water surface to the tip of the foil

<sup>9</sup> angle relative to the transverse plane

<sup>10</sup> forward edge of the main sail

Table 3: Forces and lever magnitude in the x-z plane

Force	Lever	Magnitude [m]
Driving Force	$y_{F_x}$	3.8
Total Resistance	$y_{R_f}$	1
Crew weight	$x_{W_c}$	2.2
Forward foil Lift	$x_{L_f}$	0.7
Elevator lift	$x_{L_r}$	2.7

### 2.2.3 Heave stability

The heave stability is driven by the surface-piercing<sup>11</sup> Z-foils of the Nacra 17. In fact, for a given speed, the amount of lift generated by the foils decreases as the depth immersion decreases too. Therefore, the boat will find the necessary area to keep the boat stable as the foils act as passive control systems, which are opposed to active control systems which generally use a wand system to control the flaps and therefore the angle of attack of the submerged foils. On Nacra 17, as mentioned in section 2.2.2, the angle of attack of the main foils are controlled through the pitch angle that the crew will provide depending on its longitudinal position. From the 3D model of the foils, it is possible to predict the foils' wetted area (for drag) and horizontal projected area (for lift) depending on their depth immersion. The associated graph is shown in figure 7. As the foils have

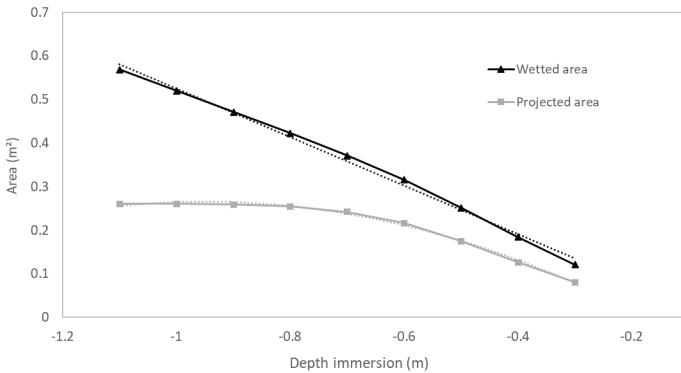


Figure 8: Total foil's wetted and projected areas relative to the depth immersion

a J-shape with an 'elbow' around half the span, the projected area decreases moderately because of their vertical part near the hull as the depth immersion decreases. In fact the projected area when the foils are fully immersed (depth immersion = 1.13 m) is 0.26 m<sup>2</sup> and decreases to a value of 0.24 m<sup>2</sup> when the tips of the foils are 0.7 m away from the design waterline. Past this 'elbow' point, the projected area decreases more rapidly and the catamaran will therefore become more unstable for the same amount of variation in heave. As expected,

<sup>11</sup>foil area changes with flight height

the wetted surface area decreases linearly with the depth immersion.

## 2.3 Performance Prediction

### 2.3.1 Overview

In a few decades, naval architecture has made a great leap forward in terms of technological advancement. In parallel with materials progress, conception tools have constantly modernized alongside computer development. According to Fabio Fossati [12], the problems of predicting the performances of a sailing boat date back to the 1930's, when the first methods for calculating boat speeds and attitude were proposed. These form the background to modern methods. Among them, Ken Davidson performed in 1936 some researches on the relation between the longitudinal and lateral resistances of sailing yacht hulls [1]. Then, in the late 1970's, a computer program was developed by Justin E. Kerwin within the Massachusetts Institute of Technology (MIT) and under the guidance of Commodore Irving Pratt, for calculating yacht performances on the basis of hull lines, rig and sail plan [24]. This project consisted in a series of elements such as a hydrodynamic model based on towing tank tests, an aerodynamic model for different Apparent Wind Angle (AWA), an optimisation procedure for finding the solution for boat equilibrium in steady state conditions and the development of a new handicap system. This was thus the first VPP and its individual components were subsequently perfected to be still used today.

Due to the complexity of predicting the performances of an unsteady yacht's motion caused by the unsteady nature of wind, one usually limits oneself to *steady state* conditions [14]. This idea which relies on the 'Kerwin method' is presented in figure 9 where a constant boat speed, heel angle and leeway angle is found when sail forces and hydrodynamic forces are in equilibrium.

More advanced methods have emerged in the past few years that evaluate the boat's performances not only in steady state conditions, but also dynamically by solving the yacht's equations of motion in a time series [14]. These methods are called 'Dynamic VPPs' (DVPP) or Performance Prediction Programs (PPP). However, this report does not investigate these approaches, which are mainly used for evaluating velocity losses due to tacking and gybing or calculating the actual fluid dynamic properties of the yacht in a time-series (further research on this method can be found in [14]). The method used in this report is therefore only based

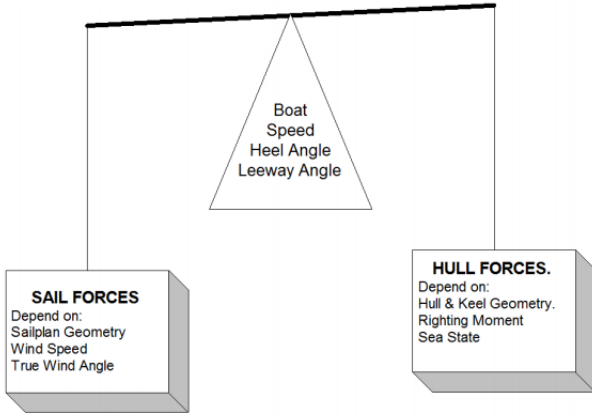


Figure 9: Equilibrium of aero and hydrodynamic forces [8]

on the steady-state conditions and the equilibrium conditions that solve the necessary equations of motions. The results are presented in the form of polar diagrams, where for a given point located on one curve, the radius corresponds to the boat speed and the angle represents the boat direction relative to the wind blowing from top to bottom.

### 2.3.2 Aerodynamic model

The role of the aerodynamic model in a VPP is to determine as accurately as possible the forces generated by the sails. There are a number of simplified approaches that have been developed in the past decades. According to Böhm [14], the first attempt to determine sail forces was performed by Davidson [1] in the 1930's where the 'Gimcrack' coefficients were obtained by measuring side force and drag on a model, combined to the full-scale model measurements to form the upwind performance prediction.

Further investigations to predict rig forces have been conducted such as wind tunnel methods, full-scale measurements and Computational Fluid Dynamics (CFD). These breakthroughs allowed to create a certain aerodynamic database for conventional VPPs that usually consists of aerodynamic coefficients (lift and drag), as functions of the apparent wind angle. These coefficients are thus stored for various single sails or set of sails. While much effort has been put into improving the aerodynamic model, most performance prediction methods used today are based on the previously mentioned 'Kerwin method' developed in 1978. Over the years, several improvements have been made until a key paper on developments of the International Measuring System (IMS) VPP of ORC was published in 1999 by Claughton [8] from the Wolfson Unit of the University of Southamp-

ton. Since then, every year, the IMS VPP undergoes subsequently improvements published by the ORC in which sail forces, in the latest versions, are represented by algorithms that are based on a combination of science and reverse engineering from the measured sailing performance of real boats [9].

For instance, the curves of the aerodynamic coefficients from this ORC database are plot in figure 10. It consists of the lift and drag coefficients,  $C_L$  and  $C_D$  respectively, of the mainsail, the jib and the spinnaker on a pole as a function of the apparent wind angle  $\beta_{AW}$ . Regarding the lift produced by the sails, there is a rapid increase until the separation sets and the sail stalls. Moreover, the various sails cover different intervals of apparent wind angles, thanks to their shape and different trim. For instance, due to the spinnaker shape, it can be seen that the peak of lift occurs at a greater apparent wind angle and is therefore used for beam reach and broad reach angles ( $90^\circ$  to  $150^\circ$  true wind angles). Finally, at apparent wind angles close to  $180^\circ$  (which in aerodynamic terms correspond to angles of attack close to  $90^\circ$ ), lift tends to drop to zero while the resistance coefficients approach unit value. [12].

Another important feature from the ORC aerodynamic model is the introduction of a depowering scheme which is mainly based on two variables: *flat* and *reef*. The *flat* parameter is used to model the plan geometry and therefore the aerodynamic behaviour of the sails. The *flat* parameter reflects the effect of flattening the sail, which as a matter of fact reduces the camber and therefore tends to decrease the lift produced as well as lower the height of the centre of effort, which reduces the heeling moment. The *reef* is used to model the variation in sail area. Though, the Nacra 17 does not have the ability to reef the sails and this parameter is therefore not computed in the mathematical model.

### 2.3.3 Hydrodynamic model

The hydrodynamic model consists of describing mathematically all the forces generated below the water surface when the boat is in motion. Various methods can be used, and recently, the use of commercial CFD solvers have drastically increased as it is one of the most accurate and precise methods for solving the hydrodynamic forces for a specific yacht. Though, due to its cost and complexity regarding its methods, other methods such as semi-empirical ones based on previous researches were used in this study. Not many researches were done on predicting the hydrodynamic performances of modern foiling catamarans, and because the Nacra

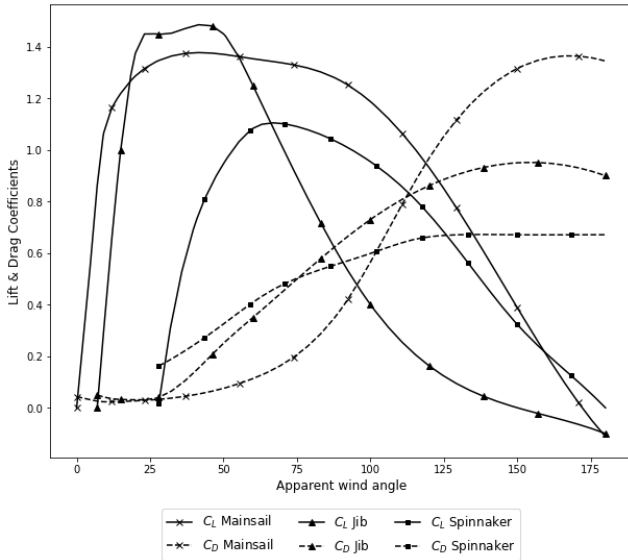


Figure 10: Sail aerodynamic coefficients

17 is a catamaran with two long slender hulls, it has very different hydrodynamic characteristics to other conventional (non-lifting) yachts. As mentioned in section 2.1.3, the hull drag can be broken down into several parts. The major contributions are the skin friction drag and the residuary resistance. The skin friction drag is due to the viscous effects which causes friction between the hull and the water. The residuary resistance (or "wave making" drag) originates from the energy lost as the hull moves through the water and creates waves. The most common used method for estimating the skin friction coefficient of a hull is the correlation-line equation developed at the 1957 International Towing Tank Conference (ITTC) [2].

Then, through the use of the 3D model, a first estimation of the hull resistance was performed using ©Maxsurf slender-body model. Hydrodynamic coefficients were obtained and then compared to the results collected in the resistance experiment completed by A.F Molland in 1994 at the University of Southampton [6] for the residuary resistance.

The appendage resistance is comprised of several components which are listed below:

- Profile Drag, composed of skin friction and pressure form drag
- Induced drag, due to the difference of pressure over a lifting end plate
- Spray drag, due to the surface piercing nature of the appendages which generate energy with the formation of spray when foiling.
- Wavemaking resistance, which includes some wavemaking effects created when the lifting surfaces are in proximity to the free surface.

These effects carry energy away from the craft in the wave train.

The role of the VPP is to find the minimum hydrodynamic drag for every boat speed and side force associated. From all the resistance contributions, the VPP first searches for the foiling conditions and optimises the parameters that are necessary for the craft to be fully supported by the lifting surfaces. Then, an optimisation function solves for the minimum drag with the constraint of remaining out of the water and keep the boat stable in the x-z plane from the equations of equilibrium described in the next section.

## 3 Mathematical Approach

### 3.1 Flow chart and numerical method

The VPP was written using Python, version 3.6 as the author has familiarity with it compared to other languages. Moreover, as a powerful tool for engineers, Python is comprised of many available packages and its concept of object-orientated programming is suited for iterative processes such as a steady-state condition VPP.

From this background, it is possible to draw a flow chart diagram (Fig 11) that summarizes the VPP process. It reflects the sequence of functions within the code and help construct the VPP based on an iterative process. In other way, it can be interpreted as the translation between the numerical language and the physical process acting in real-life. As a matter of fact, each small box in the flow chart corresponds to a number of functions implemented in Python which describe mathematically the physics that occurs in real-life. When added together, these functions allow to determine the conditions and the parameters at which the boat is in equilibrium, given a true wind speed, and a true wind direction as displayed in the first boxes of the flow chart.

As explained previously, the flow chart is comprised of two different "paths", each corresponding to the aerodynamic and hydrodynamic models. First, the aerodynamic (blue box on the left hand side in the cart) solves for the forces acting above the waterline by first determining the apparent wind data from the true wind speed, the boat speed and the heading angle. It is therefore necessary for the first iterations to input a first guess of the boat speed that will determine the initial apparent wind conditions. The closer the first guess, the faster the VPP will find the equilibrium of forces acting on the Nacra 17. From this blue box,

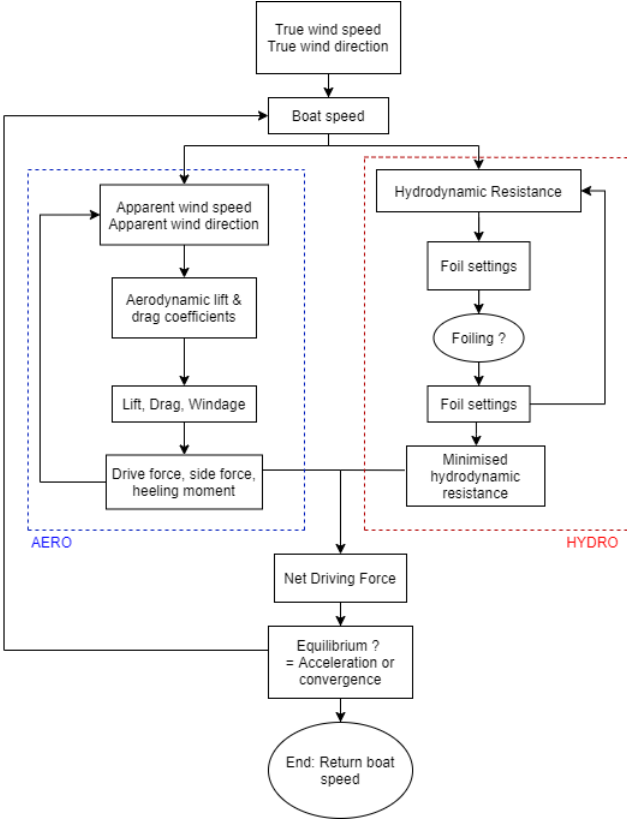


Figure 11: VPP Flow chart

the driving force, the side force and the heel angle are obtained and then compared to the red box, where hydrodynamic physics is mathematically determined. Individual resistance components need to be clearly identified in order to be as precise as possible. Most functions are based on empirical formulas described in the following section.

One of the main challenges of the VPP, transcribed in the flow chart's oval function "Foiling?", is to determine physically and numerically the conditions for which the boat can fly and therefore explain mathematically the transition from the displacement mode to the fully-foiling mode, which is explained in section 3.3.2. Once the foiling-state conditions are numerically passed, the function transcribed in the flow chart by "Foils settings" returns the minimised resistance and the associated settings such as angle of attack, depth of immersion or crew position. This function is done by using the *scipy.optimize* package provided by Python, which minimises a given objective function using "Sequential Least Squares Programming" (SLSQP), which is an iterative numerical solution of constrained nonlinear optimization problems. The function is subject to the constraints and boundaries given in section 3.3.2.

Finally, the iterative process of the VPP, as shown in the last box, is based on the acceleration of the Nacra 17 when the driving force is greater

than the overall resistance or the deceleration when the resistance is greater. This can be numerically translated by adding the percentage difference between the two forces to the previous boat speed, so that the convergence occurs when the final boat speed remains stable and meets the equilibrium conditions with a percentage difference of less than 0.1%:

$$V_{S+1} = V_S + \left( \frac{F_x - R_t}{F_x} \right) \quad (3)$$

## 3.2 Aerodynamic Model

First the Apparent Wind Speed (AWS) and direction need to be calculated to know how the sails are trimmed based on the boat speed and true wind speed and direction. Then the lift and drag forces due to the sails and structural windage are calculated, where these forces are resolved into the aerodynamic drive and side force under the constraint that the heeling moment and pitching moments may not exceed the maximum righting and pitching moments respectively calculated with the means of free-body diagrams in sections 2.1.4 and 2.2.2.

### 3.2.1 Wind triangle

Knowing that the VPP inputs are the true wind speed  $V_T$ , true wind angle  $\gamma$  and an initial boat speed guess  $V_S$ , the apparent wind angle  $\beta$  and speed  $V_A$  can be calculated (see figure 5):

$$\beta = \tan^{-1} \left[ \frac{\sin \gamma}{\cos \gamma + V_S/V_T} \right] \quad (4)$$

$$V_A = \frac{V_T \sin \gamma}{\sin \beta} \quad (5)$$

### 3.2.2 Sail Force Model

The lift  $L$  and drag  $D$  produced by the air flowing around the sails can be calculated:

$$D = \frac{1}{2} \rho_{air} S_{sail} V_A^2 C_D \quad (6)$$

$$L = \frac{1}{2} \rho_{air} S_{sail} V_A^2 C_L \quad (7)$$

where  $C_L$  and  $C_D$  are obtained from the graph 10. As mentioned in [18], the VPP assumes that each sail can be characterized by a maximum achievable lift coefficient and a corresponding viscous drag coefficient  $C_{D0}$ . Therefore, neither the induced

drag nor the pressure form drag coefficients are accounted for. So the total  $C_D$  is equal to:

$$C_D = C_{D_0} + C_{D_i} + C_{D_p} \quad (8)$$

where the induced drag, resulting from the air flowing over the leeward side due to the difference of pressure, is a function of the lift produced:

$$C_{D_i} = kC_L^2 \quad (9)$$

$$k = \frac{1}{\pi A_G} \quad (10)$$

and

$$C_{D_P} = 2C_{D_0}(1 + k) \quad (11)$$

introduces a form factor  $(1 + k)$  to the viscous drag coefficient  $C_{D_0}$  which is a function of sail's shape and materials. A form factor of 1.05 was assumed due to the finesse of the sail and the recent materials used on the Nacra 17.

The *flat* parameter is then introduced in order to reflect the effect of flattening the sails and reduce the heeling moment created by the overall aerodynamic side force and the height of the *CE*. The initial value of *flat* is 1.0 and then reduces progressively to a value of 0.62 if the forces generated are too great. A flat parameter of 0.80 means that 80% of the maximum lift is being used.

The drive and side force,  $F_x$  and  $F_y$ , can now be resolved in the boat's direction and its perpendicular direction respectively such as in figure 3:

$$\begin{cases} F_x = L \sin \beta - D \cos \beta \\ F_y = L \cos \beta + D \sin \beta \end{cases} \quad (12)$$

and the heeling moment is calculated as:

$$M_Z = F_y z \quad (13)$$

where  $z$  is the vertical distance from both centres of effort. The VPP needs to find the equilibrium in the  $z$ - $y$  plane where the righting moment created by the weight of the crew is required to get the final heel angle of the catamaran. The catamaran is fitted with two trapezes which allow the crew to be hooked outside the platform and therefore increase the lever of their contributions to the total righting moment. Several cases are considered in this report where the VPP finds the optimum number of crew needed out on the trapeze. Indeed, keeping a hull out of the water leads to a reduced hydrodynamic resistance and therefore a greater driving

force which allows the foils to generate enough lift earlier. Figure 12 is a graph showing the righting moment curves provided by the crew depending on their transverse position on the platform and an example of the heeling moment varying with the heel angle of the boat. As a matter of fact, the resulting side force in the  $z$ - $y$  plane decreases as the boat heels, as pictured in figure 4. For a matter of simplicity, the maximum heel angle is assumed to be  $12^\circ$ , where the maximum righting moment occurs. Thanks to the 3D model, it was also shown that the windward hull starts being out of the water from a heel angle of  $4^\circ$ , therefore the VPP searches for the optimum righting moment and heel angle (between 0, 1 or 2 crew on trapeze) that will oppose the heeling moment calculated previously. The moment of equilibrium on the graph occurs when the Righting Moment (RM) curve crosses the HM curve at a specific heel angle.

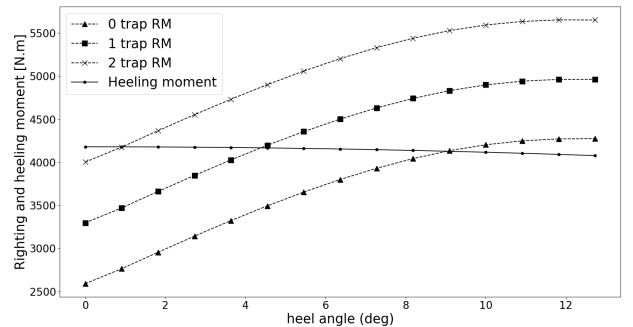


Figure 12: Righting and heeling moments vs. heel angle (example for a total crew mass of 120kg and an aerodynamic side force of 1100N)

### 3.2.3 Windage

It is of great importance to mathematically determine the aerodynamic drag of all the non-lifting parts of the catamaran as it contributes to a large component of drag when foiling. Limited literature was found on this topic but it was shown on small dinghies such as the International Moth that the aerodynamic drag can be up to 70% of the hydrofoil drag for upwind courses [11]. Basic physics and knowledge are taken from [16]. The aerodynamic is obtained by summing individual drag components as shown in equation 14.

$$D_A = \frac{1}{2} \rho_{air} V_A^2 \sum A_j C_{Dj}(\beta) \quad (14)$$

where the individuals components are the hulls, the crew, the rigging, the trampoline and the forward cross-beam. It is assumed that the mast and the boom are covered previously in the Sail Force

Model and the tiller's<sup>12</sup> contribution is neglected, as well as the emerged parts of the appendages when foiling. The area of each component being a function of the apparent wind angle, the contribution and estimations of the coefficients are based on Hoerner's research [4] following their sectional shape.

### 3.3 Hydrodynamic Model

The hydrodynamic is governed by the ability of the Nacra 17 to foil out of the water and remain stable in certain conditions. It is therefore of crucial importance to state the flying conditions and understand when the boat meets the conditions to fly and remain stable for a given wind speed and direction. It is assumed that the craft adopts whatever leeway angle necessary to produce the reaction force that counters the aerodynamic side force  $F_y$ . In real-life conditions, this hydrodynamic side force is developed by the hull and appendages in non-flying conditions and only by the appendages when flying. Though it is assumed in this study that the hydrodynamic reaction force is produced only by the daggerboards and therefore only the induced drag of the daggerboards needs to be calculated in the mathematical model.

#### 3.3.1 Hull resistance

The resistance of a single hull is estimated, neglecting the effects of wave reflection and interaction between the two hulls. In the case where the two hulls are immersed, the program simply add the respective resistance together. Though, as mentioned previously, the case where two hulls are immersed is relatively rare as the crew will minimise the drag by lifting the windward hull out of the water, which the program tries to follow. As mentioned in section 2.3.3, the hull resistance can be broken down into two main parts:

##### 1. Viscous Resistance

The ITTC skin friction correlation line to obtain the friction coefficient can be written as:

$$C_f = \frac{0.075}{(\log Re - 2)^2} \quad (15)$$

where  $Re$  is the associated hull's Reynolds number, taken as 70% of the waterline.

##### 2. Residuary Resistance

It was found that the geometry of the hull was similar to one of the model tested in towing tank in

[6]. Therefore, the residuary resistance coefficients  $C_R$  are obtained as a function of Froude number and added to the frictional resistance coefficient (i.e  $C_D = C_f + C_R$ ) in order to get the total hydrodynamic drag from the hulls. For Froude numbers higher than 1 (i.e 13.8 *knots*), the coefficients are extrapolated as the curve, past a Froude number of 0.80, decreases linearly. The total hydrodynamic drag of the hull can then be estimated as:

$$R_h = \frac{1}{2} C_D \rho_w A_w V_s^2 \quad (16)$$

where  $A_w$  is the wetted surface area of the hull obtained from the 3D-model hydrodynamic data.

#### 3.3.2 Flying condition

##### 1. Balance of vertical forces and moments

The vertical balance that needs to be satisfied is:

$$L_1 + L_2 + \Delta_e = W \quad (17)$$

where  $L_1$  and  $L_2$  are the elevators' and daggerboards' lift,  $\Delta_e$  the effective displacement and  $W$  the total weight. Once the craft becomes fully foil-borne (i.e  $\Delta_e = 0$ ),  $L_1$  and  $L_2$  must satisfy another criteria, that there is no pitching moment (as shown in figure 7):

$$L_1 + L_2 = W, \quad (18)$$

$$x_{crew} \Delta_{crew} - x_1 L_1 - x_2 L_2 = F_x z \quad (19)$$

where  $z$  is the vertical distance between the CE of driving forces and the CE of resistive forces. This system of equation therefore returns the required lift  $L_{req}$  of the forward foils.

##### 2. Appendages drag estimation and optimisation function

A first guess of lift coefficient is obtained for the forward foils by applying the following equation:

$$C_{Lfd} = \frac{L_{req}}{\frac{1}{2} \rho_w V_s^2 A_{proj}} \quad (20)$$

where  $A_{proj}$  is the total projected immersed area of the two combined forward foils. For this first guess, the two foils are assumed to be fully immersed in order to get the maximum area available. From the 3d model, the total projected area is  $0.26035m^2$ , where the following relationship applies from figure 8:

$$A_{proj} = -0.048y_{rh}^2 + 0.8386y_{rh} - 0.1332.$$

From the data of NACA-2416 profile [3],  $C_L$  is constrained between -0.2 and 1.2 for the foil not

<sup>12</sup>bar fitted to the head's rudder used for steering

to stall. A margin of 30% is applied so  $C_{Lmax}$  is limited to 0.85, which corresponds to an Angle of attack of  $10^\circ$ .

In the case where  $-0.2 < C_{Lfd} < C_{Lmax}$ , a new function is created to obtain the most optimised parameters ( $C_{Lfd}, \alpha, y_{rh}$ ) that will minimise the overall foils' drag  $D_{dagg}$ , where:

$$D_{dagg} = \frac{1}{2}\rho_w A_{wetted} V_s^2 C_D + D_{spray} \quad (21)$$

and  $A_{wetted} = 0.5576y_{rh} - 0.0315$

The lifting foil drag will comprise the profile drag of the foil section, the wavemaking drag of the foil beneath the free surface and the induced drag caused by the generation of lift. The induced drag is increased, relative to a deeply submerged foil, as a result of the free surface increasing the downwash [25]. These effects are described below.

$$C_D = C_{Dp} + C_{Di} + C_{Dw} \quad (22)$$

The coefficient of profile drag is calculated as in Hoerner [4] as a function of the friction drag based on the ITTC-57 correlation line and uses a form factor [7] to allow for the effect of pressure form drag :

$$C_{Dp} = 2(1 + k)C_F \quad (23)$$

$$(1 + k) = 1 + 2\left(\frac{t}{c}\right) + 60\left(\frac{t}{c}\right)^4 \quad (24)$$

Then, the induced drag is calculated in the same way as for the sails in equation 9, modifying the aspect ratio in 10 .

When foiling, both forward and rear appendages are losing energy by spraying water due to their surface piercing nature as they are the only components connecting the platform to the water. Yet, when in displacement mode, the rudders being hung from a gantry some distance behind the transom and the daggerboards being fully immersed, only rudders still lose energy due to the formation of spray. As a consequence, the hydrodynamic model only considers the rudders' spray drag in displacement mode and adds that of daggerboards when fully-foil borne. The amount of spray drag can then be estimated as in [5]:

$$D_{spray} = \frac{1}{2}\rho t c V_s^2 C_{D_{spray}} \quad (25)$$

$$C_{D_{spray}} = 0.009 + 0.013\left(\frac{t}{c}\right) \quad (26)$$

Finally, the wavemaking drag is usually small compared to the pressure form drag and the induced drag. Yet, it is relatively straightforward to calculate analytically the coefficient of drag and the overall contribution of the wavemaking resistance as shown below. The coefficient of wavemaking drag is related to the wave number, chord length and depth of immersion [25].

$$C_{Dw} = k_0 C_L(\alpha)^2 \quad (27)$$

$$k_0 = \frac{gc}{2V_s^2} \exp\left(\frac{-2gh}{V_s^2}\right) \quad (28)$$

where due to the negative sign, the closer a lifting foil is to a free-surface the greater the wavemaking resistance, and also the risk of ventilation. Ventilation consists of air being sucked from the atmosphere down to the lifting surface of the foil, which can cause separation, reducing the lift generated. Though, ventilation effects are not considered in this study, nor cavitation effects which arise due to the pressure in the fluid falling below vapour pressure resulting in small cavities and cause vibrations and thus a reduction in lift. The hydrodynamic model therefore constrains the depth of immersion to a minimum of  $0.7m$  for a matter of stability and cavitation.

$C_L$  being a direct function of Angle of attack  $\alpha$ , it can be approximated that for  $-0.2 < C_L < 1.2$ :

$$C_L = 0.074\alpha + 0.116 \quad (29)$$

Therefore, the total hydrodynamic drag, when foiling, can be written as a function of the angle of attack and depth of immersion of the foils, that is  $D_{dagg} = f(\alpha, y_{rh})$  and can therefore be minimised to find the optimised overall resistance:

$$\text{minimise}(D_{dagg}) \quad (30)$$

$$D_{dagg} = \frac{1}{2}\rho V_s^2 (0.5576y_{rh} - 0.0315) \quad (31)$$

$$\times \left[ 2(1 + k)C_f + \frac{C_L^2}{\pi AR} + \frac{C_L^2 gc}{2V_s^2} \exp\left(\frac{-gy_{rh}}{V_s^2}\right) \right] \quad (32)$$

with the following constraints and boundaries:

- $C_l - 0.074\alpha - 0.116 = 0$
- $C_L - \frac{L_{req}}{0.5\rho_w V_s^2 A_{proj}} = 0$
- $-0.1 < C_L < 0.85$
- $-4 < \alpha < 10$
- $0.7 < y_{rh} < 1.13$

The function will therefore return the corresponding minimised drag and an array of 5 elements:  $C_L$ ,  $\alpha$ ,  $y_r h$ ,  $V_s$ , and the lift required at the forward foil calculated previously.

### 3.4 Numerical program processing

The numerical tool developed on python is a series of functions with an iterative process. The VPP returns a DataFrame comprised of 18 columns which allows the user to understand the evolution of all the interaction of forces acting on the boat through the iteration process, until the final boat speed is found. The VPP takes 1.5 secs in average to solve for one optimum speed, given a single TWS, a single TWA and a single crew position (on a 2017 Intel(R) Core i7-7500U 2.7GHz processor). When solving for 5 TWS, a range of TWA between 25 and 180° with a 1° increment, and for 6 longitudinal crew positions, the code calculates around 2,445,000 pieces of data (forces, moments, apparent wind data, boat speed) that are directly added to the DataFrame, where each row corresponds to an iteration through the inner loops so that the analysis is straightforward and the mistakes quickly noticed. The same code loops through 4,800 final boat speeds and returns 800 of them, corresponding to the optimised boat speeds which are plotted on the polar diagram. Though, the increment of 1° in the TWA range being very time consuming, it is only used to compare the VMGs and the angles at which the boat starts flying and be as precise as possible. The polar diagrams shown in section 4.1 are plotted and interpolated with a 5° increment to reduce computational time and avoid discontinuities.

For the code to return a complete polar diagram, a computational time of approximately 1,110 seconds (18.5 minutes) is needed to solve the task, corresponding to an average value of 1.2 seconds per TWS and TWA. Therefore, minimising the computing time is of crucial importance and can be done through several ways. For instance, defining all the individual functions beforehand allows to store the data and spot the errors more conveniently. Another way to improve the computing efficiency was to interpolate all the necessary data before the final function. For instance, in the ORC VPP documentation [18], only a limited number of sail coefficients are given (10 coeffs for 10 apparent wind angles) so a greater range of apparent wind angles (with a 1° increment) was set using the *interp1d*, *cubic* function from the *scipy* package to save computational time. Another way is to use the *numpy array* package instead of using lists as it handles better mathematical operations and can

store a large amount of data. Moreover, it can read an Excel Spreadsheet where data is stored with a simple line of code.

## 4 Results & Discussions

### 4.1 Presentation of Polar Diagrams

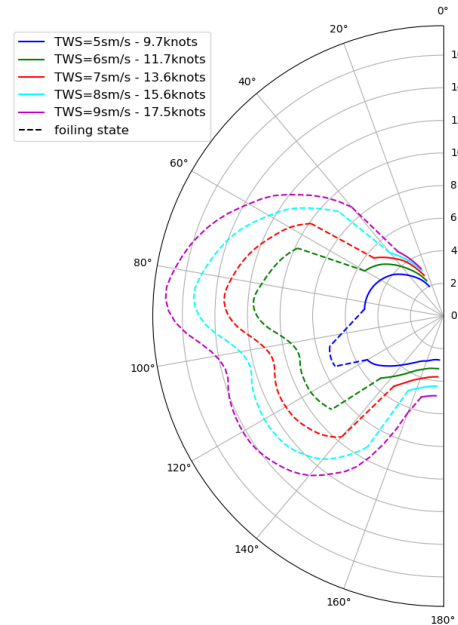


Figure 13: Nacra 17 interpolated Polar diagrams with a 150kg crew for a range of True Wind Speed between 5 and 9 m/s - with foiling state indications

The results of the performances for a crew of 150kg on a Nacra 17 are shown in figure 13. The diagram shows the interpolated curves to avoid discontinuities formed by the True Wind Angle 5° increments, as well as the wind speeds and wind angles at which the boat is foiling, indicated by the dashed lines. Several observations can be made regarding this diagram:

- i The foilborne boat speed is approximately 12 knots, as expected from the designers on their website [26].
- ii The boat starts foiling with 9.7 knots of wind, in broad reach angles, while the designers indicate a foilborne wind speed of 5 knots downwind.
- iii In upwind conditions, the foilborne windspeed is 11.7 knots, while the designers Morelli & Melvin indicate a wind speed of 12 knots.
- iv For  $TWS \geq 6$  m/s, Velocity Made Good (VMG)<sup>13</sup> are higher in a flying state mode.

<sup>13</sup>Velocity Made Good: speed of a sailboat towards (or from) the direction of the wind

- v For  $TWS \geq 6$  m/s, top speeds occur around  $90^\circ$ , reaching nearly 32 knots in 18 knots of wind speed, corresponding to the top speed predicted by the designers. Although top speeds generally occur in broad reach angles ( $110-135^\circ$ ), the VPP does not reflect this observation.
- vi Downwind VMGs occur around  $140^\circ$  for  $TWS \geq 6$  m/s.
- vii Downwind VMG for  $TWS = 5$  m/s occur at a closer TWA ( $\approx 110^\circ$ ), in a flying-state mode. A similar VMG can be achieved at a broader angle in a displacement mode ( $\approx 130^\circ$ ).

Although the present VPP recommends to bear away to reach higher upwind VMGs in foiling mode, experienced sailors rather opt for a displacement mode while sailing upwind at a closer heading angle. This foiling prediction is however of great interest as they can rapidly make a tactical decision. For instance, if the boat is being slowed by the waves such as in Keel Week in 2019, the team can opt for a foiling mode to avoid the disturbances from the waves: "teams were sailing upwind between 9.5-11 knots of boat speed [with 15-20 knots of wind]. Suddenly, after a few settings, the German team speeds up to 12.5-15 knots on their foils, flat out on the water and take a great lead." [17]. This decision remains that of the skipper and depends on several factors that the VPP cannot take into account such as the environment conditions and the other boats in the fleet.

Moreover, although top speeds generally occur in broad reach angles ( $110-135^\circ$ ), the VPP does not reflect this observation. The reason why this issue arises might be the amount of transverse force generated by the spinnaker hoisted for  $TWA \geq 90^\circ$ . As a matter of fact, the heeling forces generated are too large and therefore the flattening factor decreases the overall driving force. This comes from the difference between the aerodynamic coefficients developed by ORC for an on-pole asymmetric spinnaker and the actual shape of a Nacra 17's. Indeed, spinners on high-speed catamarans are usually much flatter, generating less drag and adapted for beam reach apparent wind angles. Therefore, the actual aerodynamic model might be more performing than that of the ORC VPP documentation. Further investigations in this area such as wind-tunnel tests with appropriate sail shapes and CFD must be carried out to get a more accurate aerodynamic force model.

Finally, performance prediction in light wind conditions ( $TWS < 5$  m/s) seems underestimated for

this type of high-performance catamaran and are not shown in this diagram as speeds do not vary between upwind and downwind conditions. These performances are compared in the next section with real-life data and other VPPs to be validated.

## 4.2 Comparison of VPP

### 4.2.1 Elapsed time on a typical windward-leeward race course

A typical race course for Nacra 17 championships such as World Championships and Olympic Games is a windward-leeward course which consists of a starting line usually perpendicular to the direction of wind with a first leg to windward followed by a leeward leg back to the start/finish line. This might be repeated with a certain number of laps to increase the race time and the number of maneuvers around windward and leeward buoys. The Nacra class usually organises the races so that they last around 30 minutes and therefore needs to predict the distance between the windward and leeward buoys, as well as the number of laps. A simple way to validate the VPP and its output VMGs is to calculate the elapsed time that the Nacra 17 would take to complete the race course. Table 4 is a table of the target time developed by the Nacra class to prepare the race course as best as possible depending on the wind strength and sea conditions. The cells colored in blue correspond to a target time of approximately 30 minutes for different wind speeds and number of laps. In parallel, the following table outlines the elapsed time calculated by the VPP to complete the race course for the associated track (i.e. in 10 knots of wind, the track would be 2 laps between buoys distanced by 1.1 or 1.2 nautical miles.). The VPP does not consider the variations in wind, so the elapsed time is calculated for all wind speeds and then compared in Table 5.

Table 4: Target time over a typical windward-leeward race course for a fleet of Nacra 17's. Available here.

Wind Range	5 - 8 Knots				8 - 12 Knots				12 - 15 Knots				15+ Knots			
	12 mins/m		6 mins/m		9 mins/m		5 mins/m		7 mins/m		3 mins/m		7 mins/m		3 mins/m	
	Up Time (mins)	Down Time (mins)														
Leg Length Nautical Miles	LA2	LA3														
0.3	10.8	16.2	3.6	1.8	7.8	11.7	2.6	1.4	6.0	9.0	2.1	0.9	6.0	9.0	2.1	0.9
0.4	14.4	21.6	4.8	2.4	10.4	15.6	3.4	1.8	8.0	12.0	2.8	1.2	8.0	12.0	2.8	1.2
0.5	18.0	27.0	6	3.0	13.0	19.5	4.3	2.3	10.0	15.0	3.5	1.5	10.0	15.0	3.5	1.5
0.6	21.6	32.4	7.2	3.6	15.6	23.4	5.1	2.7	12.0	18.0	4.2	1.8	12.0	18.0	4.2	1.8
0.7	25.2	37.8	8.4	4.2	18.2	27.3	6.0	3.2	14.0	21.0	4.9	2.1	14.0	21.0	4.9	2.1
0.8	28.8	43.2	9.6	4.8	20.8	31.2	6.8	3.6	16.0	24.0	5.6	2.4	16.0	24.0	5.6	2.4
0.9	32.4	48.6	10.8	5.4	23.4	35.1	7.7	4.1	18.0	27.0	6.3	2.7	18.0	27.0	6.3	2.7
1.0	36.0	54.0	12	6.0	26.0	39.0	8.5	4.5	20.0	30.0	7.0	3.0	20.0	30.0	7.0	3.0
1.1	39.6	59.4	13.2	6.6	28.6	42.9	9.4	5.0	22.0	33.0	7.7	3.3	22.0	33.0	7.7	3.3
1.2	43.2	64.8	14.4	7.2	31.2	46.8	10.2	5.4	24.0	36.0	8.4	3.6	24.0	36.0	8.4	3.6
1.3	46.8	70.2	15.6	7.8	33.8	50.7	11.1	5.9	26.0	39.0	9.1	3.9	26.0	39.0	9.1	3.9
1.4	50.4	75.6	16.8	8.4	36.4	54.6	11.9	6.3	28.0	42.0	9.8	4.2	28.0	42.0	9.8	4.2
1.5	54.0	81.0	18	9.0	39.0	58.5	12.8	6.8	30.0	45.0	10.5	4.5	30.0	45.0	10.5	4.5
1.6	57.6	86.4	19.2	9.6	41.6	62.4	13.6	7.2	32.0	48.0	11.2	4.8	32.0	48.0	11.2	4.8

Table 5: VMG data computed by the VPP and compared to the target times developed by the Nacra Class. Expected values in brackets.

TWS [knots]	Leg length [nm]	Expect. time [min]	VMG upwind [knots]	VMG down- wind [knots]
5-8	0.8	28.8	4.30	5.39
8-12	1.1-1.2	28.6	7.46	11.55
12-15	1.4-1.5	28.0	9.17	15.8
15+	1.5+	30	10.10	18.3
Comput. UpTime [min]	Comput. DownTime [min]	Total Computed time [min]	% difference	
11.1 (9.6)	9.0 (4.8)	40.1	+39.2	
8.8 (9.4)	5.7 (5.0)	29.0	+1.4	
8.6 (9.8)	5.3 (4.2)	27.8	-0.7	
8.9 (9.8)	4.9 (4.2)	27.6	-8.0	

It is indisputable to state from Table 5 that the performances calculated by the VPP in light winds are under-evaluated. There are a few parameters which might cause this issue and can be improved to increase the accuracy of the VPP. In light winds, one wants to reduce to a feasible extent the overall drag acting on the Nacra 17 so the present VPP must overestimate the hydrodynamic drag generated by the hulls and appendages. Compared to conventional catamarans with - or without - smaller and straight daggerboards, the Nacra 17 has a greater wetted surface area when sailing in displacement mode, and therefore a higher drag.

Moreover, the VPP being a *steady-state conditions* program, it re-iterates through all the true wind angles all the data from an initial boat speed guess without considering the momentum created by the action of bearing away which, from the acceleration, increases the apparent wind speed, and allows to generate a greater driving force. Moreover, from the hydrodynamic data run on Maxsurf, the VPP considers a single wetted surface area, whereas in light wind, the crew will move on the platform in order to reduce the wetted surface area and find the right pitch angle. The influence of the position of the crew is investigated later in section 4.3.

Finally, the aerodynamic module is based on the ORC VPP documentation [18] which obtains its sails coefficients from standard sail types and standard rig types while sails on the Nacra 17 are performance sails made of Pentex and the rig is made of standard modulus carbon fiber and cured in an autoclave. As mentioned in the previous section, the spinnaker used in the aerodynamic force model is usually hoisted on offshore racing yachts, and not

high-speed catamarans such as the Nacra 17, subject to lower apparent wind angles.

Another interesting point to notice is the similarity between the theoretical elapsed time (value in brackets in Table 5) for higher wind speeds and the elapsed time computed by the VPP following the output VMG's. As a matter of fact, for winds stronger than 8 knots, the time taken by the Nacra 17 to complete an upwind leg is smaller than the one predicted by the Class by an average of 9%. However, the time computed by the VPP for the downwind legs are slightly longer than the theoretical ones by an average of 14%, which leads to these percentage differences. The overall percentage differences for the total elapsed time around a windward-leeward course and the accuracy of the results for  $8 \leq \text{TWS} \leq 15$  (m/s) validate the results and prove that the VPP can be used by the sailors for further investigations.

#### 4.2.2 Comparison with the *Journal of Sailing Technology*

When starting the present research in September 2020, no published study was available to compare the theoretical results. In January 2021, the Society of Naval Architects and Marine Engineers published a paper written by Kai Graf (et al.) in the *Journal of Sailing Technology* describing the methods used for sail and foil trim optimization using a CFD-based VPP for the Nacra 17 [22]<sup>14</sup>. In this research flow forces are predicted using various flow analysis methods. Sail forces are taken from wind tunnel test results with a 1:5.6-scale model of the Nacra 17. Hull and daggerboard forces are derived from free-surface Reynolds Averaged Navier Stokes (RANS) flow simulations, which execute a large simulation test matrix, taking into account a range of fly-, leeway-, pitch- and heel-states, as well as velocity. The polar diagrams computed by the authors are shown in Figure 14 in the Appendix.

Several points from their analysis are held for the comparison of the two polar diagrams:

- i No transition to flying state can be observed for wind speeds lower than 5m/s.
- ii The boat starts flying on an upwind course at  $\text{TWS}=5$  m/s and  $\text{TWA}=60^\circ$ , but a higher VMG is achieved at  $\text{TWA}\approx 40^\circ$  for a displacement mode.
- iii For  $\text{TWA}\geq 6\text{m/s}$ , upwind VMGs are achieved in a flying-state mode.
- iv For  $\text{TWA}\geq 6\text{m/s}$ , boat starts flying at  $\text{TWA}=45^\circ$ .

<sup>14</sup>Only a portion of their study is used to compare both results in this paper. A deeper analysis can be found in [22].

- v For  $TWS \geq 9\text{m/s}$ , the boat loses speed because of the transverse forces being too large to meet the equilibrium conditions.
- vi Top speed predicted is approximately 27 knots in a TWS of  $10\text{m/s}$  (19.4 knots), which is, according to the designers, 15% lower than the theoretical one.

A number of similarities can therefore be found in the two polars regarding the conditions needed for the boat to fly in a stable manner, both on upwind and downwind courses. Both VPPs predict a foilborne boat speed of approximately 12 knots, and a TWS of  $5\text{m/s}$  for the boat to fly. Angles corresponding to the VMGs on a downwind course are comprised between  $120^\circ$  and  $140^\circ$ . Moreover, the issue arisen in section 4.1 concerning the transverse forces occur in both VPPs. First, the present VPP developed on Python needs to iteratively increase the speeds up to approximately 30 knots before the equilibrium of aerodynamic and hydrodynamic forces is met when  $80^\circ \leq TWA \leq 95^\circ$  and  $TWS \geq 9\text{m/s}$ . Similarly, the VPP developed by Kai Graf (et al.) using CFD encounters the same issue for  $TWS \geq 9\text{m/s}$ , where "implausible results are obtained".

Another issue encountered in their research is the jib-to-spinnaker crossover results. As a matter of fact, it can be seen in figure 14b (Appendix) that all speeds converge towards similar values for  $TWA \leq 100^\circ$ . Although, they did some wind-tunnel tests, the shape of the sails were based on that of the ORC, confirming the differences between aerodynamic models used in both VPPs and the actual force model of a Nacra 17, which was not publicly available. Though, performance prediction for beam reach angles in a typical windward-leeward race is not necessarily important as the distance to the windward spreader mark is usually short enough to allow time for the teams before hoisting the spinnaker. For each TWA, the VPP iterates through different longitudinal crew positions in order to find the optimised speed and the optimised crew setup to start foiling early and take the advantage over other teams. The following section investigates the influence of crew position as well as crew weight on the overall performances of the boat.

### 4.3 Influence of crew weight and crew position on performances

#### 4.3.1 Crew weight investigation

As mentioned in 2.1.1, on lightweight catamarans such as the Nacra 17, the mass of the crew can be

equal, perhaps higher than the boat's so the major contribution of the righting moment, as proved in 3.2.2 comes from the moment created by the crew sitting on the hull or being hooked on trapeze. Therefore, it is of crucial importance to investigate the parameters that will keep the boat in equilibrium at high speeds and help sailors understand how their behaviour on the boat influences the overall performances. Although the VPP cannot solve for the parameters dynamically in a time series, it is possible to modify its input variables and compare the different results. It was chosen to investigate the influence of three different crew weights (120kg, 150kg & 180kg).

The polar diagram corresponding to a true wind speed of  $5\text{m/s}$  for a range of true wind angles between  $60^\circ$  and  $150^\circ$  is shown in figure 15a (Appendix). It is clear to state from the graph that the lighter crew has an advantage in light winds over the heavier crews as they can fly earlier at  $TWA \approx 90^\circ$  and remain in a foiling state for a wider range of TWA up to  $TWA \approx 125^\circ$  whereas crews of 150kg has a narrower foiling window, switching from a flying mode to a displacement mode at  $TWA \approx 115^\circ$ . As a consequence, the output VMGs are markedly different: the light crew has a downwind VMG of approximately  $4.1\text{m/s}$  ( $\approx 8$  knots) while the 150kg crew has a VMG of  $3\text{m/s}$  ( $\approx 6$  knots). Over a typical windward-leeward race course with legs of  $1.1\text{nm}$ , the time difference would be about 28% between the two crews. Regarding the heavier crew of 180kg, it can be seen that the foiling-state mode cannot be achieved and has therefore a clear disadvantage over the other crews. Though, the downwind VMG is not greatly impacted compared to the 150kg crew, due to their narrow flying-state window which ends around  $115^\circ$ , a TWA closer to beam reach angle than the direction of the desired course,  $180^\circ$ .

Figure 15b (Appendix), on the other hand, reveals the impact of crew weight upon the performances in medium wind speed ( $TWS=7\text{m/s}$ ) in the case where the VPP is searching for a foiling-state mode on an upwind course. Likewise, the lighter crew is advantaged over the heavier crew regarding the wider range of true wind angles at which the boat can fly. In fact, in  $7\text{m/s}$  of wind, the 120kg can start foiling at  $TWA \approx 45^\circ$  whereas the other ones fly later at  $TWA \approx 50^\circ$ . However, past this foiling transition point at larger angles, and in a non-foiling-state mode at angles closer to  $35^\circ$ , the lighter crew has a slower speed than the other crews. This can be explained by the fact that a greater side force can be supported by the heavier

crews who can sheet in the mainsail and find a sail's angle of attack which generates more lift and less drag than that of the lighter crew. The same conclusion is deduced for stronger wind speeds, where heavier crews have a great advantage when foiling is possible, getting a wider true wind angle range than the lighter crews and being able to support a greater amount of side force.

### 4.3.2 Longitudinal crew position investigation

In addition to the weight of the crew which happens to be of significant importance in the Z-Y plane, the moment created by the product of the crew weight and the associated lever arm plays a crucial role in the stability of the boat in the X-Z plane. For a matter of simplicity, the VPP is assigned a limited number of crew positions to investigate their impact on the ability of the Nacra 17 to fly on an upwind course. The position of the crew is given by the distance between the transom and the combined centre of gravity of both sailors. The assigned values are: 0.5, 0.75, 1.0, 1.25, 1.5 and 1.75m from the transom and are shown in the graph below.

In every case, even in light winds, the VPP recommends to be located as far aft as possible between 0.5 and 0.75m from the transom. These values are not necessarily the observations reflecting real-life conditions, but one can understand in these graphs how the VPP operates. In fact, the further aft the crew, the greater the lever arm from the centre of gravity of the boat and therefore the more the catamaran can support pitching moment when foiling. In fact, when looking at figure 7 in section 2.2.2, it is explicit to state that it is mainly due to the moment created by the crew weight that the boat does not nose-dive. In addition, the further aft the crew, the greater angle of attack they can give to the daggerboards, which will in this case generate more lift and start flying earlier than other crew position. For instance, in light winds (TWS=5m/s, fig 16a in appendix), it is clear to state that the crew position at the back of the hull is advantaged over the other positions as from 1.0m onward, the catamaran cannot switch from a displacement mode to a foiling state. Similarly, in  $TWS \geq 6m/s$ , the crews being located between the transom and 0.75m away can fly from angles relatively close to the wind (40-45°). Though these observations do not necessarily correspond to reality. As a matter of fact, the VPP does not take into account the momentum of the boat and therefore the dynamic stability created by the foils, where the crew was expected to move longitudinally in order to passively control the pitch angle of the hulls.

Again, foiling on an upwind course is not necessarily of greater advantage according to experienced sailors, where they will rather opt for an efficient displacement course on which they will be located the further forward in order to keep the boat as straight as possible, along with hydrodynamic resistance and keeping the driving force parallel to the water surface. Therefore, a further dynamic investigation would be more appropriate to show the influence of crew positioning on the stability of the foiling catamaran.

## 4.4 Limitations

Although the VPP takes into account a great number of parameters and can return optimum settings, numerous topics of investigations could not be considered or can be improved for future work. The list summarizing the limitations can be found below:

- All forces are estimated using empirical formulas.
- Only rudder's elevators takes into account the effects of free surface.
- Top speeds are predicted to occur at beam reach angles, which does not reflect real-life sailing.
- Pitching moment was accounted for, but prediction of maximum PM was apparently too large as the main limited factor was the HM.
- Due to assumptions in the foils profile, validation of the actual forces around the foils is missing.
- Due to computing time limitation, only a limited number of crew weights and crew positions were investigated which did not allow to get more precise results.
- Deflection, ventilation and cavitation of the foils were neglected.
- The water surface was assumed to be flat, no study in waves or other disturbances was achieved.
- Sail force model is based on ORC documentation, originally assigned for offshore yachts.
- Twist in the mainsail is neglected.
- Wind velocity and wind direction gradients were neglected.
- Flying height is constrained to avoid foil stall and implausible results in the optimisation function for foil's drag.
- The momentum of the boat was neglected.

A deeper investigation of the Nacra-17's behaviour based on numerical methods can be conducted using more advanced tools such as CFD and

wind-tunnel tests on scaled-models such as in [22] to improve the accuracy of the results and keep aiding sailors in their training for the next Olympic Games and World Championships.

## 5 Conclusion

A steady-state Velocity Prediction Program for the mixed-crew Olympic Class foiling Nacra 17 was developed on Python and used to investigate the influence of different crew setups, including the crew weights and the longitudinal positions. The aim was to develop a numerical tool that helps sailors find the optimum setup rapidly among the numerous different options. The results are analysed in terms of VMGs and capacities for the Nacra-17 to foil and therefore gain speed.

The parameters playing a role in the overall performances were therefore assessed and implemented in the code. An aerodynamic model describing the forces acting above the waterline was developed based on the ORC VPP documentation and a hydrodynamic model describing the forces generated by the action of the water flowing on the different immersed surfaces was developed based on empirical formulas and optimisation functions. The VPP iteratively solves for the speed of the Nacra-17 and indicates the foiling-state conditions with the associated crew setup. Crew weights of 120, 150 and 180kg were investigated, as well as their longitudinal positions: from 0.5m to 1.75m away from the transom. It was found that light crews of 120kg are advantaged in light winds ( $\leq 5m/s$ ) over the others as they have a wider range of headings at which the Nacra 17 is able to fly above the water surface, and therefore drastically gain in speed, increasing their VMGs. However, these crews are disadvantaged in stronger winds as their maximum righting moment is not as high as that of crews of 180kg, which can withstand a greater aerodynamic force and therefore gain in power and speed. The foiling-state conditions were also investigated depending on the position of the crew on the Nacra 17. It was found that the Nacra 17 starts flying at headings closer to the wind when the crew is far aft, avoiding nose-diving and allowing the foils to get a greater angle of attack. Due to the steady-state conditions, the VPP cannot assess dynamically the influence of positioning on the stability of the foiling platform, and therefore only returns the most optimised position at which the Nacra 17 can start foiling and withstand more power.

The VPP was validated by simulating the time

that a Nacra-17 would take to complete a typical windward-leeward race course depending on the wind speed and compare it with real-life sailing data from the Nacra Class. It was found that the VPP was predicting very low speeds in the light winds ( $TWS \leq 4m/s$ ), where foiling is not possible. The prediction in stronger winds ( $\geq 4m/s$ ) is however more appropriate as percentage differences do not exceed 8%. The results were then compared to polar diagrams obtained from a study performed using CFD and wind-tunnels tests where similar results concerning the foiling-state conditions are found, as well as the challenges encountered when writing the code. This tool is thus designed for Nacra-17 sailors who want to understand how the foiling catamaran behaves in steady-state conditions. Further work can be done to improve the accuracy of the results and tests in real conditions can be performed to associate the theoretical data with experimental results.

## AUTHOR'S BIOGRAPHIES

**Louis Huchet** is a Master Student at the School of Engineering Sciences, in Maritime Engineering & Ship Science, at the University of Southampton. His research interests include yacht aero and hydrodynamics and engineering applications in high performance sport.

## Acknowledgement

I would like to thank my tutor and individual project supervisor **Professor Stephen R. Turnock** of the Engineering and the Environment Faculty at the University of Southampton. Pr. Turnock was prompt in responding to all my emails and was always available whenever I had any queries and issues with my research. He allowed this project to be my own research, but was there to guide me when he thought necessary. With his support I was able to take this project beyond its original aim.

## References

- [1] K. Davidson. "Some Experimental Studies of the Sailing Yacht". In: *Transaction of SNAME* 44 (1936). Stevens Institute of Technology, Experimental Towing Tank, Hoboken, New Jersey.
- [2] "Proceedings of the 8th International Towing Tank Conference, ITTC'57". In: Report No. P1957-2. Madrid, Spain, 1957.
- [3] F.W. Riegels. *Aerofoil Sections: Results from Wind-tunnel Investigations, Theoretical Foundations*. lccn: nun00487843. Butterworths, 1961.
- [4] S.F Hoerner. *Fluid-Dynamic Drag*. Hoerner, 1965.
- [5] Richard B. Chapman. "Spray Drag of Surface-Piercing Struts". In: AIAA/SNAME/USN Advanced Marine Vehicles Meeting. Annapolis, MD, 1972.
- [6] A.F Molland, J.F Wellicome, and P.R Couser. *Resistance Experiment on a Systematic Series of High Speed Displacement Catamaran Forms: Variation of Length-Displacement Ratio and Breadth-Draught Ratio*. Ship Science Report No. 71. University of Southampton. Mar. 1994.
- [7] A.R. Claughton, A. Sheno, and J.F. Wellicome. *Sailing Yacht Design - Theory*. Addison Wesley Longman, 1998.
- [8] A. Claughton. "Development in the IMS VPP Formulations". In: SNAME 14th Chesapeake Sailing Yacht Symposium. Annapolis, 1999.
- [9] Fabio Fossati, Sara Muggiasca, and Viola. "An investigation of aerodynamic force modelling for IMS rule using wind tunnel techniques". In: 19th HISWA Symposium on Yacht Design and Yacht Construction. Amsterdam, Jan. 2006.
- [10] S. Bayraktar, Y. Ozdemir, and T. Yilmaz. "Computational analysis of wind velocity and direction effects on a sail." In: June 2007.
- [11] Bill Beaver and John Zselezky. "Full Scale Measurements on a Hydrofoil International Moth". In: The 19th CHESAPEAKE SAILING YACHT SYMPOSIUM. Annapolis, Maryland, USA, Mar. 2009.
- [12] F. Fossati. *Aero-hydrodynamics and the Performance of Sailing Yachts: The Science Behind Sailing Yachts and Their Design*. Adlard Coles Nautical, 2009. ISBN: 9781408113387.
- [13] C. Bertrand. *Comment marchent les voiliers*. Voiles et Voiliers, 2014. ISBN: 9782916083698.
- [14] C. Böhm. "A Velocity Prediction Procedure For Sailing Yachts With A Hydrodynamic Model Based On Integrated Fully Coupled RANSE-Free-Surface Simulations". PhD thesis. Delft University of Technology, Maritime Technology, Promotor Prof. R.H.M. Huijsmans., 2014.
- [15] Pete Melvin. "NACRA17-MKII Update configuration". In: Sept. 2016.
- [16] L. Marimon-Giovanetti et al. "Development of a Hydrofoiling Experimental Research Platform". University of Southampton, Faculty of Engineering and the Environment, 2017.
- [17] *On Hyperspeed, Woman Overboard, and the meaning of 'Steep Learning Curve'*. 2019. URL: <https://nacra17.org/on-hyperspeed-woman-overboard-and-the-meaning-of-steep-learning-curve/>. (accessed: 23.04.2021).
- [18] Offshore Racing Congress (ORC). "ORC VPP Documentation". In: 2019.
- [19] J.I.R Blake. *Lecture notes on SESS3027 Yacht & High Performance Craft*. Faculty of Engineering and Physical Sciences, University of Southampton, 2021.
- [20] Nacra 17 Class and Melvin P. *Curved foils, Letter on the Nacra 17 by designer Pete Melvin*. 2021. URL: <https://nacra17.org/class-info/curved-foils/>.
- [21] Nacra17 Class. *Nacra 17*. 2021. URL: <https://nacra17.org/nacra17/>.
- [22] Kai Graf et al. "VPP-Driven Sail and Foil Trim Optimization for the Olympic NACRA 17 Foiling Catamaran". In: *Journal of Sailing Technology* 5.01 (Jan. 2021), pp. 61–81. ISSN: 2475-370X.
- [23] S. Hascilowicz. *LFoilGen-etc*. 2021. URL: <https://github.com/Maselko/Lfoilgen-etc>.
- [24] J.E Kerwin and H. Irving Pratt. *A Velocity Prediction Program for Ocean Racing Yachts Revised to June, 1978*. No. 78-11. SNAME, Massachusetts Institute of Technology, MIT, Department of Ocean Engineering, Ocean Race Handicapping Project.
- [25] Anthony F. Molland and Stephen R. Turnock. *Marine Rudders and Control Surfaces, Chapt.4, 2nd edition*. to be published in 2021. Elsevier Ltd.
- [26] *Nacra 17 Specifications - Morrelli amp; Melvin: Multihull Design Engineering Brokerage*. URL: <http://www.morrellimelvin.com/n17/specs.html>. (accessed: 23.04.2021).

## 6 Appendix

### Nacra 17 performance predictions from the Journal of Sailing Technology

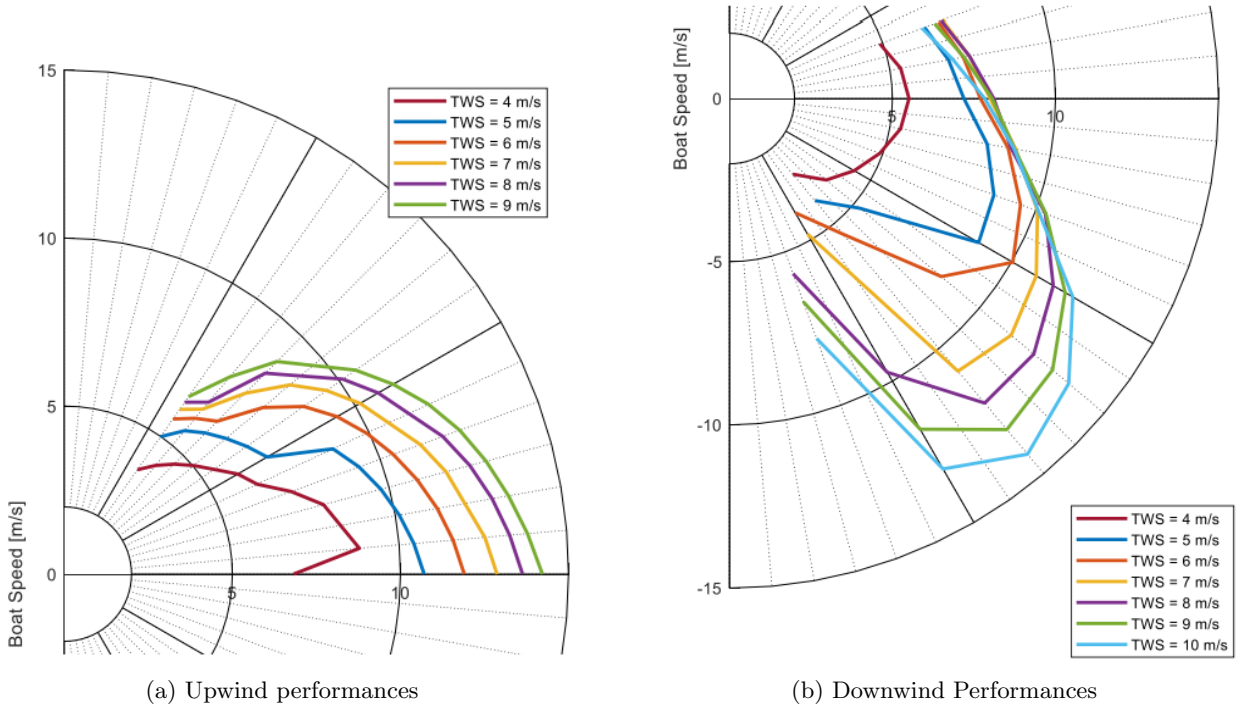


Figure 14: Nacra 17 performance predictions from the *Journal of Sailing Technology* [22]

### Crew Weight Influence on Performances

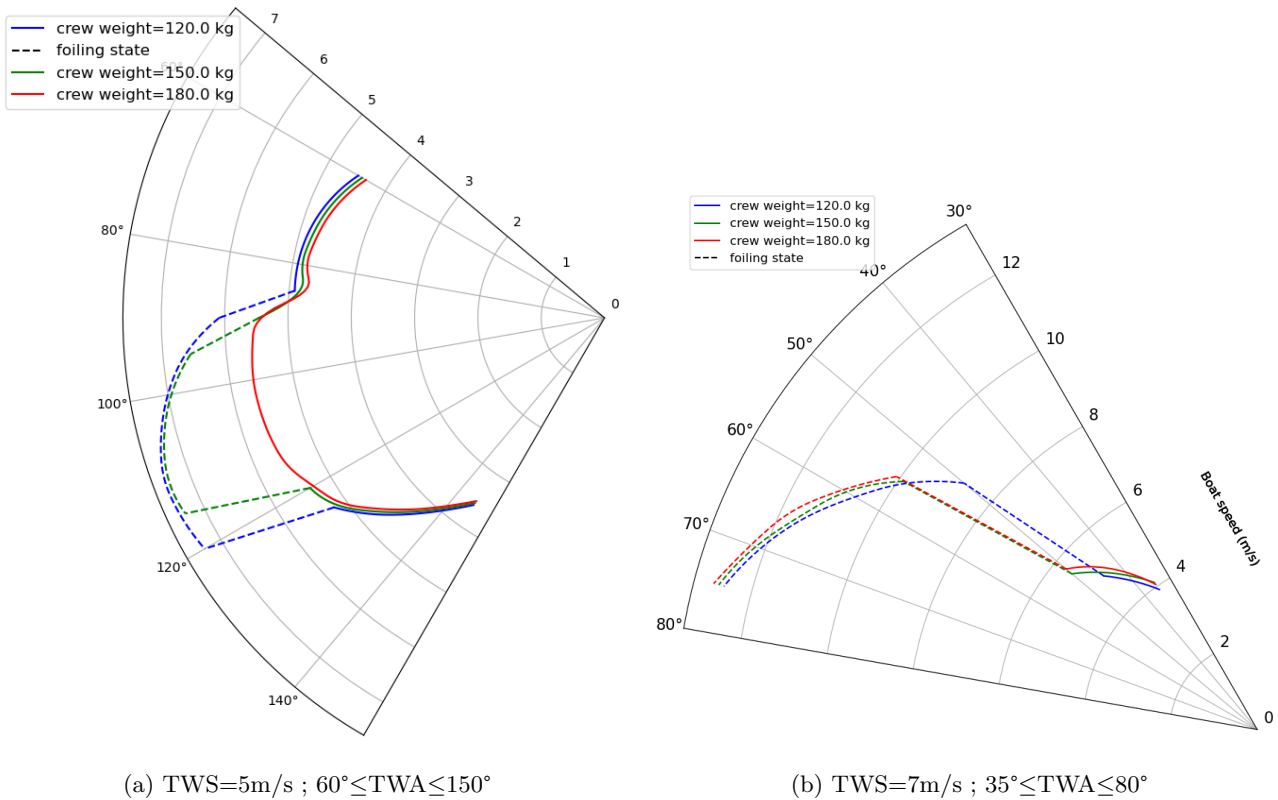
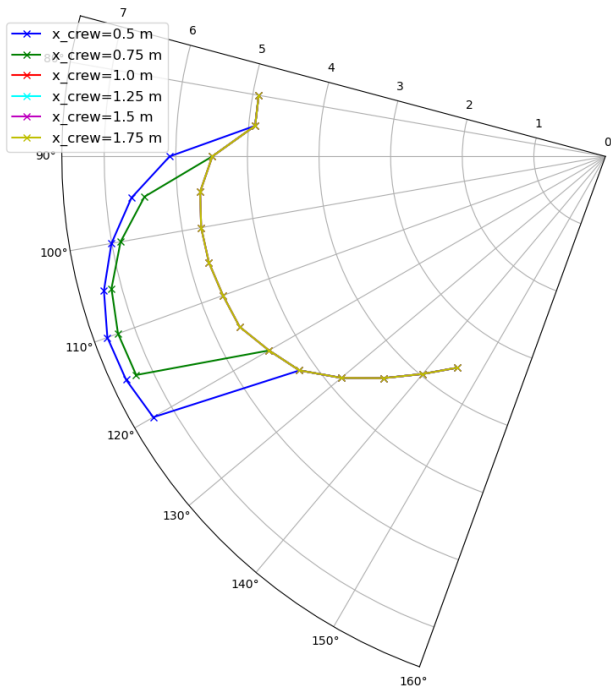
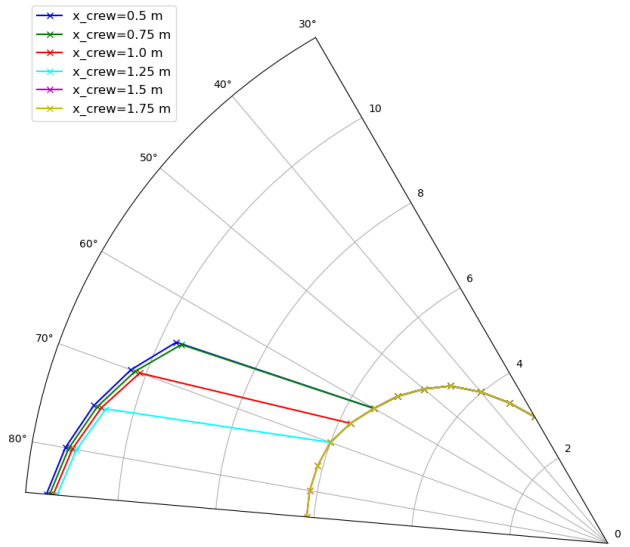


Figure 15: Comparison of 3 different crew weights (120, 150 & 180kg) in light and medium winds for a specific range of TWA.

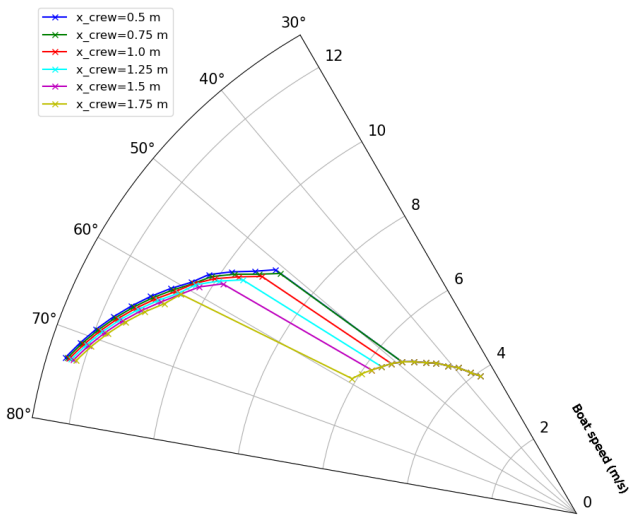
# Crew Position Influence on Performances



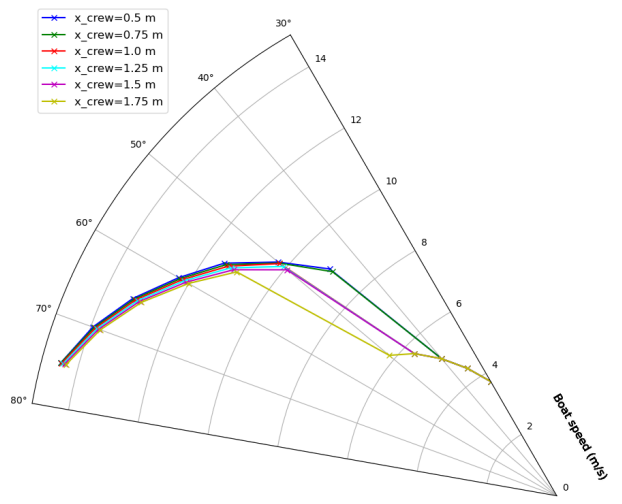
(a) TWS=5m/s ;  $80^{\circ} \leq TWA \leq 150^{\circ}$ ;



(b) TWS=6m/s ;  $35^{\circ} \leq TWA \leq 85^{\circ}$



(c) TWS=7m/s ;  $30^{\circ} \leq TWA \leq 80^{\circ}$



(d) TWS=8m/s ;  $30^{\circ} \leq TWA \leq 80^{\circ}$

Figure 16: Comparison of different longitudinal crew positions for TWS=5, 6, 7 & 8 m/s, for a crew of 150kg